# Dalton Transactions

Accepted Manuscript






ROYAL SOCIETY OF CHEMISTRY

www.rsc.org/dalton

Journal Name

ARTICLE

# Crystal Phase Competition by Addition of Second Metal Cation in Solid Solution Metal-Organic Frameworks.

Received 00th January 20xx,
Accepted 00th January 20xx

DOI: 10.1039/x0xx00000x

www.rsc.org/

C. Castillo-Blas,[a] N. Snejko,[a] V. A. de la Peña-O'Shea,[b] J. Gallardo,[a] E. Guitérrez-Puebla,[a] M. A. Monge,[a*] F. Gándara[a*].

Herein we report a synthetic study focused on the preparation of solid-solution metal-organic frameworks, MOFs, with the use of two kinds of linkers. In particular, we have explored the system composed by zinc, cobalt, 1,2,4-triazole and 4,4'-hexafluoroisopropylidenbisbenzocid acid ($H_2$hfipbb). During this study, four new MOFs have been isolated, denoted TMPF-88 [$M_3$(hfipbb)$_2$(triazole)$_2H_2O$], TMPF-90 [$M_2$(triazole)$_3$($OCH_3CH_2$)], TMPF-91 [$M_2$(hfipbb)(triazole)$_2$] and TMPF-95 [$M_5$(hfipbb)$_4$(triazole)$_2$($H_2O$)], (TMPF = transition metal polymeric framework, M = Zn, Co, or mixture of them). The study demonstrates that the addition of a second metal element during the MOF synthesis has a major effect in the formation of new phases, even at very high Zn/Co metal ratios. Furthermore, we show that during the MOF reaction formation, there is a competition among different crystal phases, where kinetically favoured phases of various compositions crystallize in short reaction times, precluding the obtaining of the pure solid-solution phases of other energetically more stable MOFs.

## Introduction

Metal-organic frameworks, MOFs, are a class of materials constructed by the assembly of metal cations and organic linkers into extended, ordered structures.[1] Traditionally, MOFs are built by the combination of one kind of inorganic secondary building unit, SBU, and one kind of organic linker to form well-defined networks; it is also possible to build MOFs with multiple linkers or building units of different geometry or connectivity, which are occupying specific positions in the framework.[2] Currently, there is a great interest in the development of MOFs that are able to display heterogeneity and disorder along with the order inherent to their crystalline nature. MOFs with these features are able to show new emerging properties, or enhancement of know ones.[3] The combination of heterogeneity and order can be afforded following different strategies, such as combination of different SBUs and/or linkers, combination of multiple functional groups,[4] introduction of defects,[5-9] pore modification, etc.

On the other hand, many properties exhibited by MOFs, such as gas adsorption selectivity,[10, 11] catalytic activity,[12] or electrical conductivity[13, 14] largely depend on the metal element that is incorporated in the SBUs. In many cases, a MOF structure type can be prepared with a just a metal element or a very limited number of them. Thus, in these cases the introduction of a desired element into a targeted MOF structure is only achievable by following a post-synthetic metal exchange, allowing the total or partial replacement of the metal cations. The cation exchange process in MOFs has been recently reviewed,[15] and some SBUs and metal coordination environments that are more suitable to undergo this process have been identified. Recently, it has also been demonstrated that it is possible to selectively remove part of the metal cations and linkers of a MOF to produce vacancies at defined sites,[16] which can be subsequently occupied by a different metal cation. Alternative to metal-exchange, it is also possible to incorporate a mixture of different metal cations into a desired MOF in a one pot synthesis. With this strategy, it is possible to prepare multi-metal or solid-solution MOFs where different cations are occupying the same crystallographic position. MM-MOF-74 appears as a notable example of solid solution MOF, which can be prepared with a mixture of 2, 4, 6, 8 and 10 different metal elements, including some elements that cannot afford MOF-74 by themselves (Ba, Ca, Sr).[17] Rare-earth based MOFs are also known to be susceptible of being prepared as solid solution MOFs, since lanthanide elements can easily replace one another. Here, the introduction of different rare-earth elements into a same framework results in the modification of the luminesce properties of the MOFs.[18] It is also expected that the introduction of multiple cations within a same SBU might result in modification of the materials properties such as catalytic activity.[19] Recently, we have shown that it is possible

[a] Department of New Architectures in Materials Chemistry – Instituto de Ciencia de Materiales de Madrid, CSIC, Sor Juana Inés de la Cruz 3, Cantoblanco, Madrid 28049, Spain. E-mail: gandara@icmm.csic.es, amonge@icmm.csic.es
[b] IMDEA Energy Institute, Móstoles Technology Park, Av. Ramón de la Sagra 3, 28935 Móstoles, Madrid, Spain

† Electronic Supplementary Information (ESI) available: Additional characterization including PXRD patterns, ICP-CHN-EDX analyses, sorption isotherm, FT-IR and TG analyses. Crystallographic information in the form of CIF files. See DOI: 10.1039/x0xx00000x

to prepare a series of isostructural MOFs with group 13 elements, Al, Ga and In, as well as solid solution mixtures containing Ga and In at different ratios.[20] Remarkably, modification of the Ga/In ratio in the resulting solid solution MOFs provides control on the catalytic activity of the materials in complex multicomponent reactions carried out in one-pot. However, it is still unclear which are the most important factors that drive the introduction of different metal cations into a single crystalline phase, rather than producing phase segregation, and thus, to what extend it possible to prepare solid-solution MOFs of a given structure. In work here presented, we have carried out a synthetic study that involves the combination of zinc and cobalt with two different linkers, with the aim of understanding how the synthesis conditions led to the formation of a desired phase with a mixture of metal elements randomly distributed in the inorganic SBUs.

In particular, we have combined the dicarboxylic 4,4'-hexafluoroisopropyliden-bis-benzocid acid and 1,2,4-triazole along with zinc and cobalt, two metal elements that typically exhibit similar coordination environment. As a result, we have obtained four new MOFs (scheme 1), denoted TMPF-88, TMPF-90, TMPF-91 and TMPF-95 (TMPF = transition metal polymeric framework). The introduction of two kinds of linkers results in a complex system with multiple possible combinations of reactants. Thus, our study demonstrates that the introduction of a second cation in the synthesis media significantly modifies the reaction system, resulting in the appearance of competing crystalline phases, which might even undergo phase transformation. Our results illustrate the importance of synthesis variables such as pH and solvents in the formation of desired solid solution MOFs, where a mixture of metal cations can be disorderly incorporated into the SBUs. Furthermore, we show that the value of the metal cation ratio added in the synthesis drastically influences the appearance of new phases, and that under certain conditions the incorporation of a second cation can only be achieved at trace level.

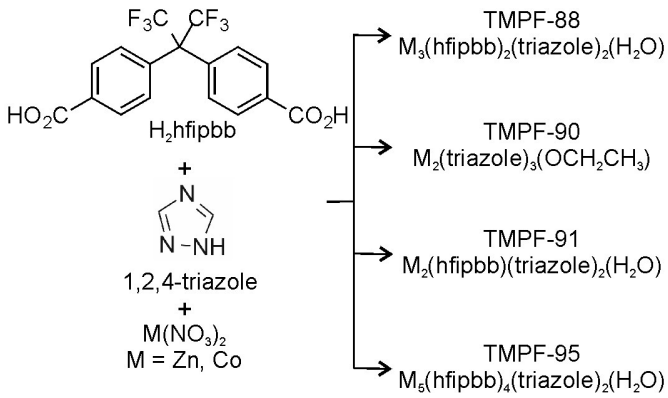


**Scheme 1**: Combination of the 4,4'-hexfluoroisopropylidenebisbenzoic acid ($H_2$hfipbb), 1,2,4-triazole and zinc and cobalt nitrate salts results in the formation of four new MOFs. In the MOF formulae, M might stand for Zn, or a mixture of Zn and Co at various ratios, as explain in the text.

## Experimental

### General information

All reagents and solvents employed were commercially available and used as received without further purification: 4,4'-hexafluoroisopropylidene-bis-(benzoic acid), $H_2$hfipbb (98% ABCR GmbH&Co); 1,2,4-triazole, (≥99% Fluka); zinc nitrate, $Zn(NO_3)_2{\cdot}6H_2O$ (≥99% Scharlab) and cobalt nitrate, $Co(NO_3)_2{\cdot}6H_2O$ (≥99% Sigma Aldrich).

Powder X-ray diffraction (PXRD) patterns were collected with a Bruker D8 diffractometer, equipped with a copper source operated at 1600W, and a position sensitive detector. Patterns were collected with a step size of 0.02° and an exposure time of 0.5 s/step.

Single crystal X-ray data were obtained in a Bruker four circle kappa-diffractometer equipped with a Cu INCOATED microfocused source, operated at 30 W power (45 kV, 0.60 mA) to generate Cu Kα radiation (λ=1.54178 Å), and a Bruker VANTEC 500 area detector (microgap technology). Diffraction data were collected exploring over a hemisphere or a quadrant of the reciprocal space in a combination of ϕ and ω scans to reach a resolution of 0.85 Å, using a Bruker APEX2 software suite. Unit cell dimensions were determined for least-squares fit of reflections with I>5σ. Space group determination was carried out using XPREP. The structures were solved by direct methods. The final cycles of refinement were carried out by full-matrix least-squares analyses with anisotropic thermal parameters of all non-hydrogen atoms. The hydrogen atoms ware fixed at their calculated positions using distances and angle constraints. All calculations were performed using APEX2 software for data collection and SHELXTL[21] and OLEX2-1.2[22] to resolve and refine the structure.

Elemental analyses were measured in an ECO CHNS-932 analyzer.

Scanning electron microscopy (SEM) images and energy dispersive X-ray spectra (EDS) were collected with a S-3000N microscope, equipped with an ESED detector and a INCAx-sight of Oxford Instruments, respectively. All samples were prepared for SEM and EDS by dispersing the material onto a double sided adhesive conductive carbon tape that was attached to a flat aluminum sample holder and were metallized with a gold layer of 12 nm with a Quórum Q150T-S sputter.

$N_2$ sorption isotherms were measured with an AUTOSORB-1 from Quantachrome Instruments at 77K in the relative pressure range of $10^{-6}$ to 1 atm. Before adsorption measurements, the samples were activated by solvent exchange with methanol (15 mL, 3 times exchanged over a 2 days period) and outgassed at 408 K overnight.

The thermogravimetric and differential thermal analyses were collected with SDT Q600 from TA instruments equipment in a temperature range between 45 and 700 °C in air (100mL/min flow) and a heating rate of 10 °C/min.

IR spectra were recorded from KBr pellets in the range of 4000-350 $cm^{-1}$ on a Nicolet FT-IR 20SXC spectrometer.

### Computational Details

Plane-wave density functional (PW-DF) calculations were done using the VASP package.[23, 24] The energy was calculated employing the generalized gradient approximation, in particular, the exchange and correlation functional of Perdew and Wang (PW91).[25, 26] The effect of the core electrons on the valence electron density was described by the projector augmented wave (PAW) method.[27, 28] The cutoff for the kinetic energy of the plane waves was set to 415 eV throughout, which after extensive tests proved to ensure a total energy convergence better than $10^{-6}$ eV. Geometry optimization was carried out using a gradient-conjugate method. The formation energy ($\Delta E_{Form}$) was calculated as the difference between the corresponding energies of the reagents and MOF structures.

**General synthetic conditions**

**Preparation of TMPF-88, $M_3(hfipbb)_2(triazole)_2(H_2O)$**. General procedure for Zn-TMPF-88: a mixture of $H_2$hipbb (130 mg, 0.33 mmol), 1,2,4-triazole (75 mg, 1.09 mmol), $Zn(NO_3)_2{\cdot}6H_2O$ (100 mg, 0.34 mmol) in 5 ml of distilled water and 5 ml of absolute ethanol was stirred at room temperature for 5 minutes. The resulting mixture was placed in a Teflon-lined steel autoclave and heated at 170 °C overnight. After cooling to room temperature, colourless crystals were filtered off and washed with distilled water, ethanol and acetone. Yield 61% (79 mg). Elemental analysis, %weight found (calculated): C, 40.95 (39.51); H, 2.20 (2.01); N, 6.78 (7.27). TMPF-88 was also obtained as pure phase with mixture of Zn and Co with synthesis carried out with the amounts shown in table 1, entries 3, 4, 5 and 6.

**Preparation of TMPF-91, $M_2(hfipbb)(triazole)_2(H_2O)$.** General procedure with an initial 10:1 Zn:Co molar ratio: a mixture of $H_2$hfipbb (130 mg, 0.33 mmol), 1,2,4-triazole (75 mg, 1.09 mmol), $Zn(NO_3)_2{\cdot}6H_2O$ (91 mg, 0.31 mmol), $Co(NO_3)_2{\cdot}6H_2O$ (9 mg, 0.03 mmol) and a mixture of ethanol:water (5ml/5ml) was stirred at room temperature for 10 minutes. To the resulting mixture 300 µL of an aqueous 1M solution of $HNO_3$ was added to adjust the pH to ~2.5 and the reaction was placed in a Teflon-lined steel autoclave and heated at 170 °C overnight. After cooling at room temperature colourless crystals were filtered off and washed with distilled water, ethanol and acetone. Yield 36% (41 mg). Elemental analysis, %weight found (calculated): C, 38.11 (37.42); H, 2.37 (1.94); N, 12.25 (12.47). TMPF-91 was also obtained as pure phase for synthesis reactions carried out with the amounts shown in table 1, entries 1 and 2.

**Preparation of TMPF-95, $M_5(hfipbb)_4(triazole)_2(H_2O)$.** A mixture of $H_2$hfipbb (130 mg, 0.33 mmol), 1,2,4-triazole (60 mg, 0.87 mmol), $Zn(NO_3)_2{\cdot}6H_2O$ (33 mg, 0.11 mmol), $Co(NO_3)_2{\cdot}6H_2O$ (65 mg, 0.22 mmol) and 10 ml of distilled water was stirred at room temperature for 5 minutes. The resulting mixture was placed in a Teflon-lined steel autoclave and heated at 170 °C for 3 days. After cooling to room temperature, purple crystals were filtered off and washed with distilled water, ethanol and acetone. Yield 61% (102 mg). Elemental analysis, weight% found (calculated): C, 42.87 (42.87); H, 1.94 (1.90); N, 4.51 (4.57).

**Preparation of TMPF-90, $M_2(triazole)_3(OCH_3CH_2)$.** General procedure with an initial 4:1 Zn:Co molar ratio: a mixture of 1,2,4-triazole (69 mg, 1 mmol), $Zn(NO_3)_2{\cdot}6H_2O$ (24 mg, 0.08 mmol), $Co(NO_3)_2{\cdot}6H_2O$ (6 mg, 0.02 mmol) and a mixture of ethanol:water (3ml/3ml) was stirred at room temperature for 10 minutes. The resulting mixture was heated at 90 °C overnight. After cooling to room temperature, yellow powder was filtered off and washed with distilled water, ethanol and acetone. Yield 73% (9 mg). Elemental analysis, weight% found (calculated): C, 24.09 (23.29); H, 1.81 (1.67); N, 35.91 (38.80). TMPF-91 was also obtained as pure phase for synthesis reactions carried out with the amounts shown in table 1, entries 7, 8, 9 and 10.

**Table 1**. Optimized synthetic conditions for the obtaining of pure samples. Temperature = 170 °C, and reaction time = 18h

| Entry | Initial amounts | | | | | Experimental | |
|---|---|---|---|---|---|---|---|
| | $H_2$hfipbb mg, mmol | 1,2,4-triazole mg, mmol | $Zn(NO_3)_2$ mg, mmol | $Co(NO_3)_2$ mg, mmol | $H_2O$:EtOH | phase | Formula[a] |
| 1 | 130, 0.33 | 75, 1.09 | 100, 0.34 | - | 5ml:5ml | TMPF-91 | $Zn_2(hfipbb)(triazole)_2$ |
| 2 | 130, 0.33 | 75, 1.09 | 91, 0.31 | 9, 0.03 | 5ml:5ml | TMPF-91 | $Zn_{1.90}Co_{0.10}(hfipbb)(triazole)_2$ |
| 3 | 130, 0.33 | 75, 1.09 | 100, 0.34 | - | 5ml:5ml | TMPF-88 | $Zn_3(hfipbb)_2(triazole)_2(H_20)$ |
| 4 | 130, 0.33 | 60, 0.87 | 91, 0.31 | 9, 0.03 | 10ml:0ml | TMPF-88 | $Zn_{2.98}Co_{0.02}(hfipbb)_2(triazole)_2(H_20)$ |
| 5 | 130, 0.33 | 60, 0.87 | 80, 0.27 | 19, 0.07 | 10ml:0ml | TMPF-88 | $Zn_{2.96}Co_{0.04}(hfipbb)_2(triazole)_2(H_20)$ |
| 6 | 130, 0.33 | 60, 0.87 | 67, 0.23 | 33, 0.11 | 10ml:0ml | TMPF-88 | $Zn_{2.96}Co_{0.04}(hfipbb)_2(triazole)_2(H_20)$ |
| 7 | - | 69, 1.00 | 6, 0.02 | 24, 0.08 | 3ml:3ml | TMPF-90 | $Zn_{0.86}Co_{1.14}(triazole)_3(CH_3CH_2O)$ |
| 8 | - | 69, 1.00 | 17, 0.05 | 17, 0.05 | 3ml:3ml | TMPF-90 | $Zn_{1.10}Co_{0.90}(triazole)_3(CH_3CH_2O)$ |
| 9 | - | 69, 1.00 | 24, 0.08 | 6, 0.02 | 3ml:3ml | TMPF-90 | $Zn_{1.21}Co_{0.79}(triazole)_3(CH_3CH_2O)$ |
| 10 | - | 69, 1.00 | - | 34, 0.10 | 3ml:3ml | TMPF-90 | $Co_2(triazole)_3(CH_3CH_2O)$ |
| 11[b] | 130, 0.33 | 60, 0.87 | 33, 0.11 | 65, 0.22 | 10ml:0ml | TMPF-95 | $Zn_{1.84}Co_{3.16}(hfipbb)_4(triazole)_2(H_2O)$ |

[a]Formula determined by elemental and ICP analyses. [b]Reaction time = 3 days

**Crystal structure descriptions**

A summary of the crystal and refinement data for the new MOFs is given in table 2.

TMPF-88, $Zn_3(hfipbb)_2(triazole)_2(H_2O)$. The compound crystallizes in the monoclinic *C*2/*c* space group. There are three crystallographically independent zinc atoms in the asymmetric unit, all of them in tetrahedral coordination environment. The Zn atoms are coordinated to three triazolate anions and six carboxylate groups from the hfipbb linkers. A water ligand completes the coordination sphere of Zn2. Additionally another water ligand with partial occupancy was located at 2.67 Å from Zn3. The position of Zn3 could actually be split in two positions, so that this atom is partially found in tetrahedral environment and in trigonal bypiramidal environment when there is presence of this additional water ligand. The occupancy for the two positions of Zn3 was refined to a 51:49 ratio.

The inorganic SBUs consist of three metal cations (Figure 1A). They have a linear shape and are disposed along the *c* axis. Triazolate and hfipbb linkers connects the SBUs to form a three dimensional framework, with channels running along the *c* axis (Figure 1B). The channels are of 8.8 by 8.4 Å dimensions. $N_2$ sorption isotherm shows that TMPF-88 is permanently porous, with a BET surface area of 120 $m^2g^{-1}$ (190 $m^2g^{-1}$ Langmuir).

TMPF-91, $Zn_2(hfipbb)(triazole)_2$. The compound crystallizes in the monoclinic *Cc* space group. There are two crystallographically independent Zn atoms in the asymmetric unit. One of them is in tetrahedral coordination environment, coordinated to two nitrogen atoms from the triazolate linkers, and to two oxygen atoms, one from a carboxylic group from hfipbb and the other one is a water ligand. The second Zn atom is pentacoordinated, with square pyramidal environment. The coordination sphere is made of four nitrogen atoms from triazolate anions, and one oxygen atom from a carboxylic group from a hfipbb linker. The Zn atoms are connected along the *a* and *c* axis by triazolate anions (Figure 2A), while the $hfibpp^{2-}$ anions connect the metal cations along the *b* axis. The resulting three-dimensional structure is densely packed, with no open space (Figure 2B).

**Table 2**. Crystal and refinement data for TMPF-88, TMPF-90, TMPF-91 and TMPF-95

| | Compound **TMPF-88** | Compound **TMPF-90**[a] | Compound **TMPF-91** | Compound **TMPF-95** |
|---|---|---|---|---|
| Formula | $C_{38}H_{23}F_{12}N_6O_{10.46}Zn_3$ | $C_8H_6N_9OZn_2$ | $C_{21}H_{13}F_6N_6O_5Zn_2$ | $C_{72}H_{38}Co_5F_{24}N_6O_{17.48}$ |
| Molecular Weight/ g $mol^{-1}$ | 1155.12 | 374.97 | 674.11 | 2017.37 |
| Temperature/K | 296 (2) | 296 | 296 (2) | 233 (2) |
| Wavelenght/Å | 1.54178 | 1.54056, 1.54439 | 1.54178 | 1.54178 |
| Crystal system | Monoclinic | Orthorombic | Monoclinic | Monoclinic |
| Space group | *C*2/*c* | *Pnma* | *Cc* | $P2_1/n$ |
| a/Å | 36.4551(9) | 7.598(7) | 10.0888(4) | 14.8692(5) |
| b/Å | 18.1156(4) | 10.016(6) | 33.8241(11) | 24.8713(8) |
| c/Å | 14.1588(4) | 17.457(8) | 7.0903(2) | 22.1361(7) |
| α/° | 90 | 90 | 90 | 90 |
| β/° | 93.8165(13) | 90 | 96.002(2) | 91.621(2) |
| γ/° | 90 | 90 | 90 | 90 |
| V/$Å^3$ | 9329.8(4) | 1328.7(5) | 2406.26(14) | 8183.0(5) |
| Z | 8 | 4 | 4 | 4 |
| Dx/ g $cm^{-3}$ | 1.645 | 1.809 | 1.861 | 1.638 |
| μ/$mm^{-1}$ | 2.789 | | 3.328 | 83887 |
| F (000) | 4597.0 | | 1340.0 | 4011.0 |
| GOF $F^2$ | 1.082 | | 1.182 | 1.013 |
| Final R índices | $R_1$ = 0.0410 | Rp = 2.34% | $R_1$ = 0.0410 | $R_1$ = 0.0776 |
| [I>2sigma(I)] | $wR_2$ = 0.1307 | Rwp = 3.43% | $wR_2$ = 0.1137 | $wR_2$ = 0.1994 |
| R índices | $R_1$ = 0.0521 | | $R_1$ = 0.0518 | $R_1$ = 0.1298 |
| (all data) | $wR_2$ = 0.1613 | | $wR_2$ = 0.1451 | $wR_2$ = 0.2400 |

[a]Rietveld refinement against PXRD data

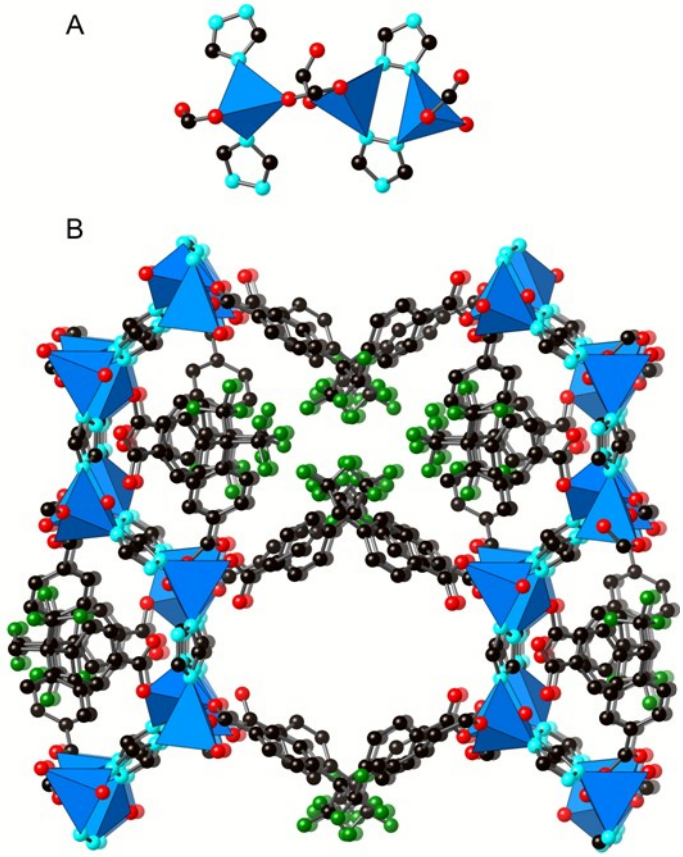


**Figure 1**. A) The inorganic SBU in TMPF-88 is composed of three linearly disposed tetrahedral metal cations. B) Depiction of TMPF-88, viewed along the *c* axis. Carbon is black, oxygen is red, fluorine is green and nitrogen is cyan. Blue polyhedra represent metal (Zn, Co) cations. Hydrogen atoms are omitted for clarity.

TMPF-95, $Co_{5-x}Zn_x(hfipbb)_4(triazole)_2$. The compound crystallizes in the monoclinic $P2_1/n$ space group, in the form of prismatic crystals with intense pink color. There are five crystallographically independent metal atoms, three of them in tetrahedral coordination environment, and the other two ones in octahedral environment. The inorganic SBUs are U-shaped, consisting of five metal cations, which are coordinated to eight carboxylic groups and to four triazolates, with a total coordination number of twelve (Figure 3A). As we explain below, the metal cations were assigned as cobalt during the crystal structure refinement, although elemental analysis indicates presence of zinc. The positions of these two elements were indistinguishable in the structure, indicating that they must be disorderly occupying the five metal positions of the framework. The coordination of the SBUs through the organic linkers results in a three dimensional structure with a calculated 10.5% of accessible void space (Figure 3B).

TMPF-90, $Zn_2(triazole)_3(CH_3CH_2O)$ only appears as a microcrystalline powder. A small single crystal was obtained in a synthesis carried out with a mixture of $Zn(acetate)_2$, 1,2,4-triazole and $H_2hfipbb$ in a 1:3:1 molar ratio, heated at 150 °C for 18h.

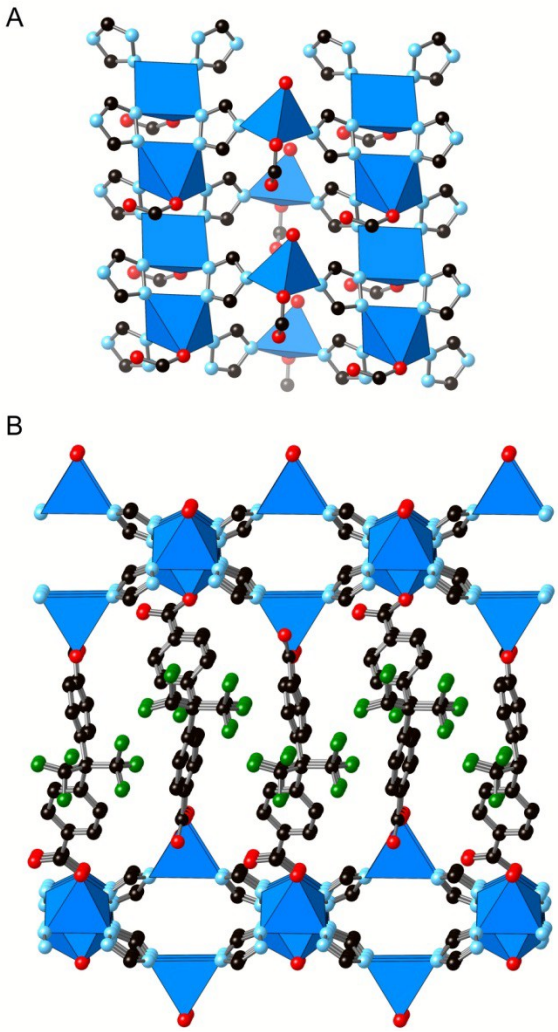


**Figure 2**. A) The inorganic SBU in TMPF-91 can be depicted as rods of metal cations, which are linked by triazolate anions. B) Representation of the three dimensional structure of the TMPF-91 along *c* axis. Layers depicted in A are perpendicular to the figure, and are connected by $hfipbb_2$ linkers. Carbon is black, oxygen is red, fluorine is green and nitrogen is cyan. Blue polyhedra represent metal (Zn, Co) cations. Hydrogen atoms are omitted for clarity.

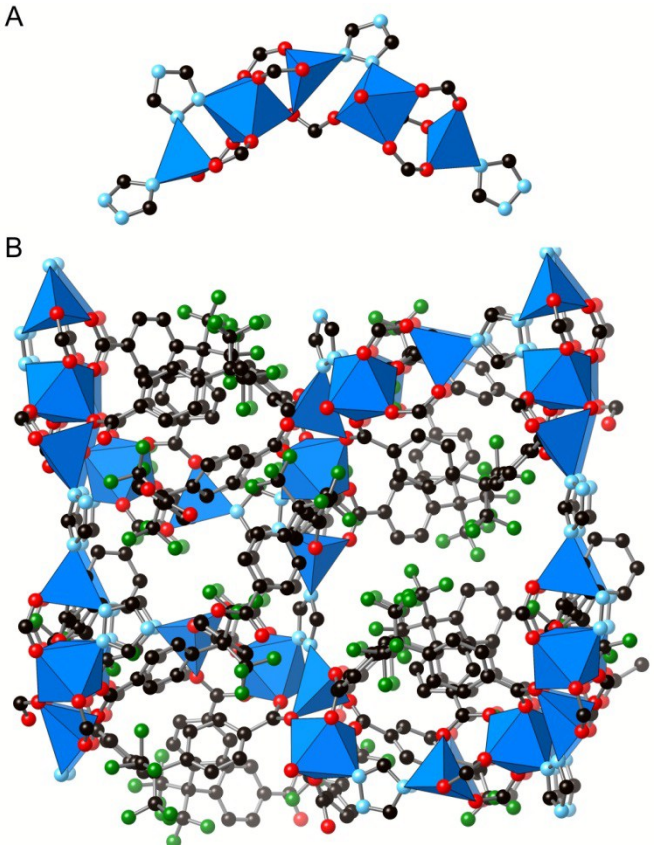


**Figure 3**. A) The inorganic SBUs in TMPF-95 are composed of five V-shaped disposed polyhedral metal cations. B) Representation of three dimension structure of TMPF-95. Carbon is black, oxygen is red, fluorine is green and nitrogen is cyan. Blue polyhedra represent metal (Zn, Co) cations. Hydrogen atoms are omitted for clarity.

However, the small size of the crystal and its poor diffracting quality precluded from completing a full diffraction data collection. Nevertheless, with data collected up to 1.1 Å and 49.3% completeness, it was possible to obtain the unit cell parameters and an initial set of atomic coordinates. The experimental PXRD patterns and the one calculated with this data set are in good agreement, and a Rietveld refinement was then carried out to confirm the correctness of the crystal structure, with final refinement indicators being Rwp = 3.71%, Rp = 2.55% (Figure S4). The compound crystallizes in the orthorhombic Pnma space group. There are two crystallographically independent metal atoms, one in tetrahedral and the other in octahedral coordination environment. The octahedral centers are exclusively coordinated to N atoms from the triazolate anions, while in the tetrahedral centers, there are only three N atoms. The fourth coordination site is occupied by an O atom coming from the ethanol solvent molecules, which should be deprotonated to account for the charge balance. The metal centers are linked through the 1,2,4-triazolate anions, such as the nitrogen atoms in position 4 of the triazole ring coordinate to the tetrahedral cations, while nitrogen atoms in positions 1 and 2 coordinate to the octahedral cations. Each tetrahedral cation is thus linked to six octahedral cations, which are disposed forming rods along the a axis (Figure 4).

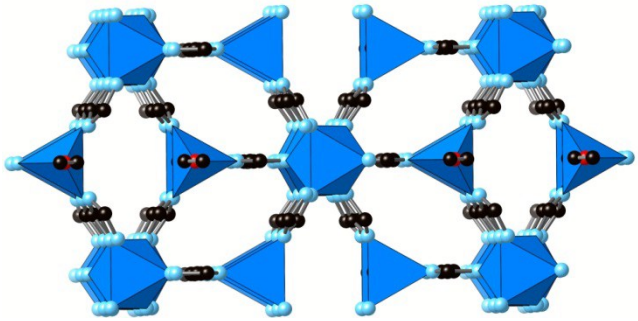

**Figure 4**. Structural representation of TMPF-90 viewed along *a* axis. Carbon is black, oxygen is red and nitrogen is cyan. Blue polyhedra represent metal (Zn, Co) cations. Hydrogen atoms are omitted for clarity.

## Result discussion

The combination of zinc nitrate with 1,2,4-triazole and $H_2$hfipbb in a 1:3:1 ratio resulted in the obtaining of Zn-TMPF-88. Initially, we carried out the synthesis using water as only solvent. Zn-TMPF-88 was isolated as pure phase as shown by PXRD, although with a low yield, a fact that we attributed to the low solubility of $H_2$hfipbb in water, since a large amount of unreacted linker remained in the reaction media. The use of a water:ethanol solvent mixture in a 1:1 ratio greatly improved the yield. With these optimized conditions, we then attempted to introduce cobalt in the structure by adding cobalt nitrate in the reaction media at the various Zn:Co ratios of 10:1, 8:1, 4:1, 2:1, 1:1, 1:2 and 0:1. The measured pH of the synthesis initial mixtures was fixed with 1M NaOH to a value of 3.5. This is the same pH value measured in the reaction carried out exclusively with zinc nitrate as the only metal salt. The phase diagram for the obtained products under these conditions is shown in figure 5. It should be noted that the conditions for the obtaining of pure phases were further optimized and are listed in Table 1.

Surprisingly, the addition of cobalt even at the lowest 10:1 and 8:1 Zn:Co ratios precludes the formation of TMPF-88, resulting in the appearance of a different phase, TMPF-91. Pale pink microcrystalline powders were obtained in both cases, whose PXRD patterns are in agreement with the calculated one for TMPF-91 (Figure S5). SEM images show plate like crystals as major phase, although it is also observed the presence of a small amount of smaller particles without well-defined shape (Figure 6A). EDS analyses were performed on different areas of the crystals to determine whether cobalt was actually incorporated into the structure. The results indicate that cobalt is indeed present in the structure, although the quantified amount of cobalt is much lower than the one initially added. Furthermore, the Zn:Co ratio is not constant

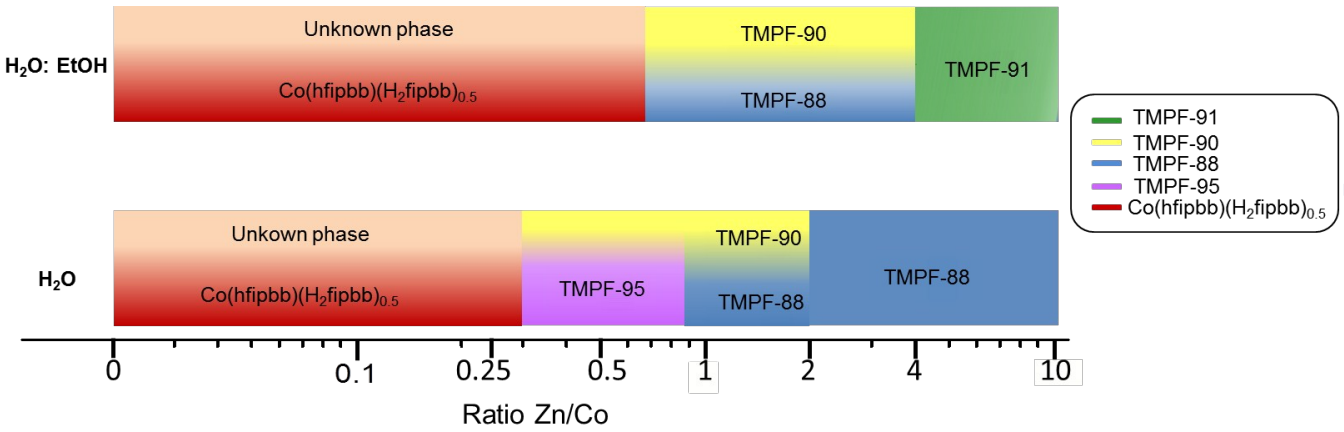


**Figure 5.** The phase diagram for the obtained products with varying Zn/Co ratios, in two different conditions: water:ethanol (up) and water (down). For all experiments, temperature was 170 °C, and heating time 18h. The Zn/Co ratio is shown in logarithmic scale, indicating the values that were investigated.

along the crystals. For the sample prepared with an initial 10:1 ratio, the Zn/Co ratios observed in three different areas of a same crystal are 34.0, 26.7 and 26.6. In the case of sample prepared with an initial 8:1 Zn:Co ratio the differences are even larger, with observed Zn/Co ratios of 21.9, 20.9 and 45.7 (Figure 6). Although experimental error associated to variations in beam penetration in a tilted sample cannot be completely ruled out, these results seem to indicate that the incorporation of cobalt into the structure is not homogeneous, and therefore the MOF composition varies along the crystal. This is also in agreement with differences in composition previously observed for multi-metal MOF-74.[17]

When we increase the amount of cobalt in the reaction to 4:1, 2:1, and 1:1, TMPF-88 is obtained in the form of large crystals with pale pink colour (crystal size largest dimension around 500 µm). However, the MOF now appears mixed with a yellow microcrystalline powder, which is actually formed by needle-like microcrystals (5µm), as observed in the SEM images (Figure 7A). This powder was identified as TMPF-90, according to the PXRD pattern (Figure S9). EDS analysis carried out for crystals of TMPF-88 prepared with an initial 2:1 Zn:Co ratios demonstrate that cobalt is included in the MOF. Similar to the previous observation, the amount of cobalt incorporated is substantially lower than the amount initially added. Besides, the distribution of cobalt also varies along a same crystal, as shown by the measurements performed in different areas of the same crystal. The Zn/Co ratios are in the range between 24 and 15, measured in three areas from three different crystals (Figure 7B). Since TMPF-90 only contains 1,2,4-triazole as organic linker, we attempted to obtain TMPF-88 as a pure phase by decreasing the amount of triazole in the reaction media, which otherwise is added in excess (1.09 mmol). However, in all reactions with an amount of 1,2,4-triazole between 1.09 and 0.80 mmol, TMPF-90 is always present. Furthermore, if the amount of 1,2,4-triazole is lower than 0.80 mmol, TMPF-88 is no longer formed.

In another effort to separate both phases, we then studied the kinetic of this reaction system, by collecting the PXRD patterns of the products obtained after reaction times of 1h, 2h, 3h, 4h, 6h, 8h and 18h (Figure 8). After 1 hour of heating, only unreacted $H_2$hfipbb linker is present in the PXRD pattern.

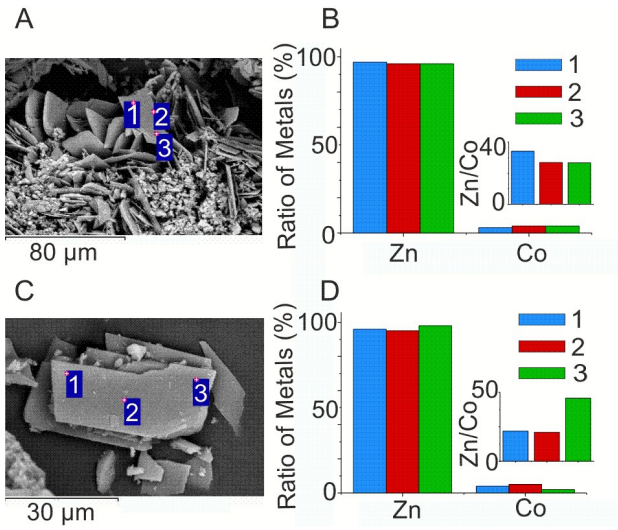


**Figure 6**. SEM images corresponding to TMPF-91 crystals, indicating the areas where the EDS analyses were performed. A) Sample prepared with an initial 10:1 Zn:Co ratio. B) Plot of the ratio of metals (%) and Zn/Co ratio (inset) determined by EDS analysis, where each column corresponds to the area indicated by a number in panel A. C) Sample prepared with an initial 8:1 Zn:Co ratio. D) Plot of the ratio of metals (%) and Zn/Co ratio determined by EDS analysis, where each column corresponds to the area indicated by a number in panel C.

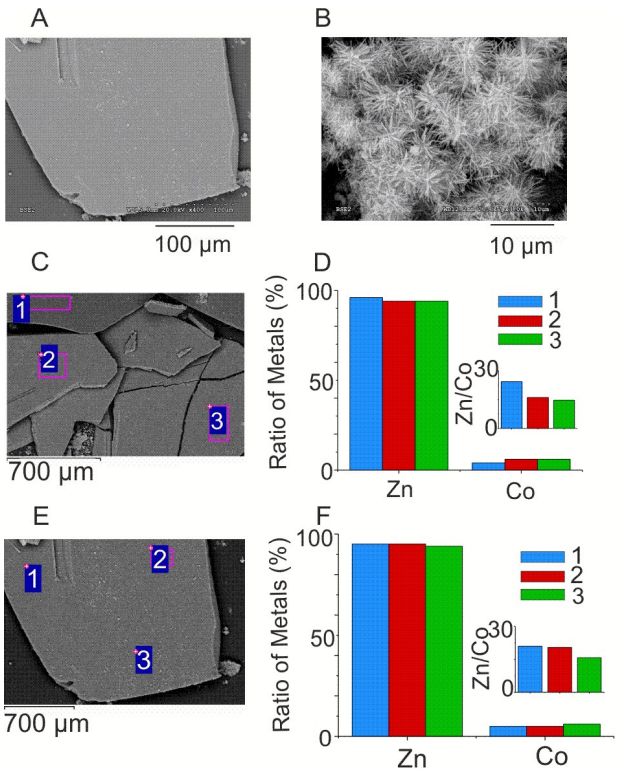


**Figure 7**. SEM images corresponding to TMPF-88 crystals, indicating the areas where the EDS analyses were performed A) SEM images of two areas corresponding to sample prepared with an initial 2:1 Zn:Co ratio showing a crystal of TMPF-88 and B) microcrystals of TMPF-90. C) SEM image showing TMPF-88 crystals corresponding to a sample prepared with an initial 2:1 Zn:Co ratio, indicating the points were the EDS analyses were performed. D) Plot of the ratio of metals (%) and Zn/Co ratio determined by EDS analysis, where each column corresponds to the area indicated by a number in panel C. E) Sample prepared with an initial 2:1 Zn:Co ratio and shows points of the same crystal. F) Plot of the ratio of metals (%) and Zn/Co ratio determined by EDS analysis, where each column corresponds to the area indicated by a number in panel E.

Interestingly, after 2 hours the PXRD pattern indicates the formation of an additional crystalline phase, which was identified as a MOF with composition Zn(hfipbb), which was previously reported by us, and hereon we denote as ZnPF-1.29 TMPF-90 appears after 3 h heating, mixed with ZnPF-1. It seems reasonable to think that the formation of ZnPF-1 results in a higher relative concentration of triazole in the reaction solution, therefore favouring the formation of TMPF-90. After 4 hours heating, the presence of TMPF-88 is already identified in the PXRD pattern, although still mixed with TMPF-90 and ZnPF-1. After 8 h heating, the intensities of the diffraction peaks corresponding to both ZnPF-1 and TMPF-90 drastically decrease. Visual inspection of the product under the optical microscope still shows presence of a yellowish microcrystalline powder typical of TMPF-90, along with large plate-like crystals of TMPF-88, suggesting that TMPF-90 is only partially re-dissolved. At this point, ZnPF-1 seems to be completely re-dissolved, as it is no longer observed in the PXRD pattern nor visually under the microscope. Interestingly, after longer reaction times (18 h), the intensities corresponding to TMPF-90 peaks increase again, being the final product a mixture of TMPF-88 and TMPF-90. To gain more insight on the formation of the different phases involved in the reaction, we estimated the structural stability of crystal phases and their synthesis mechanism during the MOF crystallization by means of theoretical calculations.[30-34] In this work, formation energies were calculated ($\Delta E_{Form}$) using the VASP package. The geometry optimization was determined using the experimental structures obtained by X-ray diffraction and always converged to a stable structure even though no symmetry constraints were imposed. The results of these calculations show that TMPF-90 and ZnPF-1 have very similar formation energies, much lower than that of TMPF-88, which is energetically more stable (Figure 9).

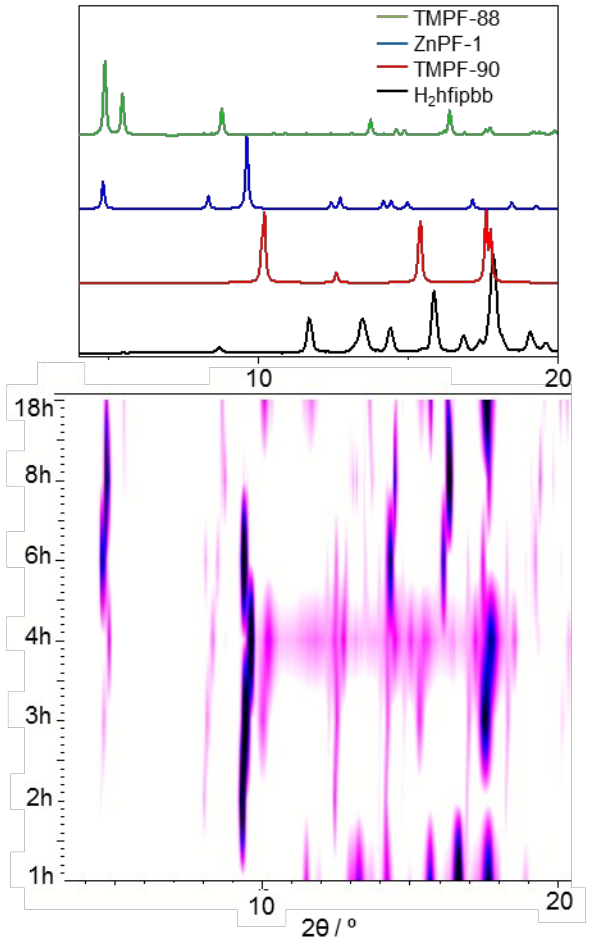


**Figure 8**. Two-dimensional plot of the PXRD patterns corresponding to the samples obtained at different reaction times. The composition of the initial synthesis mixture is 130 mg, 0.33 mmol of $H_2$hfipbb; 75 mg, 1.09 mmol of triazole; 67 mg, 0.23 mmol of $Zn(NO_3)_2$ and 33 mg, 0.11 mmol of $Co(NO_3)_2$ in all cases. The simulated PXRD patterns of the phases involved in the kinetic study are shown in the top of the figure, as a guide to the eye.

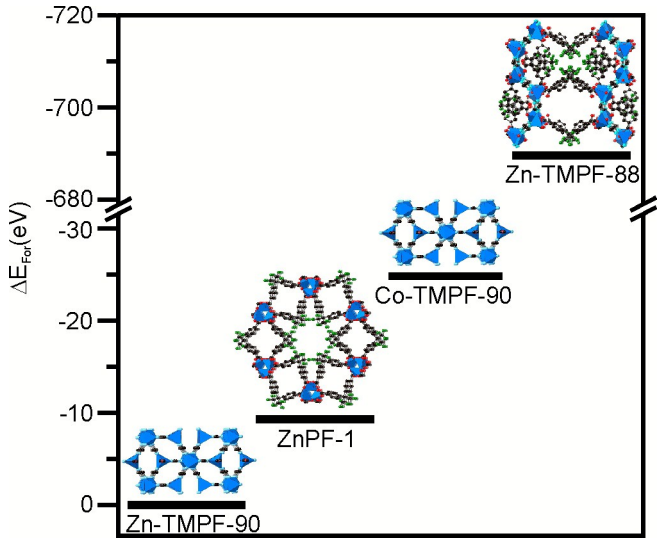


**Figure 9.** Relative formation energies for the phases involved in the kinetic study. $\Delta E_{Form}$ values have been normalized to the most stable phase.

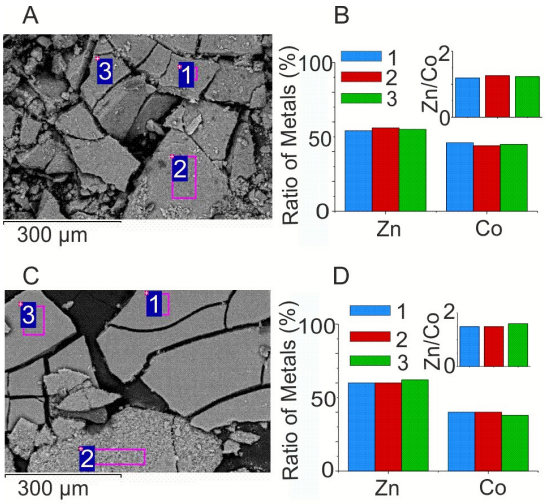


**Figure 10.** SEM images corresponding to TMPF-90 crystals, indicating the areas where the EDS analyses were performed. A) Sample prepared with an initial 1:1 Zn:Co ratio. B) Plot of the ratio of metals (%) and Zn/Co ratio determined by EDS analysis, where each column corresponds to the area indicated by a number in panel A. C) Sample prepared with an initial 4:1 Zn:Co ratio. D) Plot of the ratio of metals (%) and Zn/Co ratio determined by EDS analysis, where each column corresponds to the area indicated by a number in panel C.

In the case of ZnPF-1 and TMPF-90, the calculations were performed assuming that zinc is the only metal present. However, taking into account that TMPF-90 can be obtained independently with both zinc and cobalt (*vide infra*), we performed two calculations for this phase, one considering zinc as only metal element present (Zn-TMPF-90), and the other one with cobalt as only metal element (Co-TMPF-90). This study shows that Co based structure presents a higher stability than the Zn one. These results suggest that the inclusion of Co in the bimetallic TMPF compounds might lead to a stabilization of their structures. Thus, small differences were observed in the case of TMPF-90 depending on the metal element included, although it is likely that the actual product is composed by both zinc and cobalt, being the formation energy order ZnTMPF-90 > ZnPF-1 > CoTMPF-90. Nevertheless, these calculations support the experimental observations of the kinetic study, demonstrating that in the mixed-metal system with multiple kinds of linkers, kinetically favoured phases are readily formed, and consequently the composition and concentration of the synthesis media is not homogeneous during the MOF formation reaction.

TMPF-90 can be readily obtained with various Zn:Co ratio (4:1, 1:1, 1:4 and 0:1) as pure phase when $H_2$hfipbb is not added to the synthesis and carrying out the reaction at 90 °C. EDS analyses indicate that in this phase the Zn:Co ratio is homogeneous along the sample. For the sample prepared with a 1:1 ratio, the Zn/Co ratios obtained in three different areas of sample are 0.55:0.45. In the case of the sample prepared with a 4:1 ratio, a similar Zn/Co ratio is found in three areas of the sample (0.6:0.4), suggesting a preference for the introduction of cobalt over zinc in this structure (Figure 10).

If the Zn/Co ratio lies below 1 and the amount of cobalt is larger than that of zinc, TMPF-88 is no longer formed. For syntheses with Zn:Co ratios 1:2, 1:4, 1:10 and 0:1, crystals corresponding to a previously reported MOF[35] with formula Co(hfipbb)($H_2$fipbb)$_{0.5}$ are formed, along with a yellowish powder, whose crystal phase could not be identified. EDS analysis indicates a large percentage of nitrogen and absence of fluorine in this solid, suggesting that it might correspond to a different crystalline form of cobalt-triazolate.

Initial synthesis experiments had showed that Zn-TMPF-88 could be obtained with the use of water as only solvent, although with a low yield. We therefore also decided to perform synthesis reactions with mixture of zinc and cobalt in absence of ethanol. Syntheses carried out with water as the only solvent result in a different phase diagram, shown in bottom part of figure 5. Thus, in absence of ethanol, TMPF-91 is no longer observed for any of the Zn:Co explored ratios. TMPF-88 can be obtained as pure phase, according to PXRD and SEM analysis, for various Zn:Co ratios of 10:1, 4:1 and 2:1. However, ICP analyses of the samples indicate that cobalt is present only in trace amounts (0.10%Co, 16.86%Zn for 149 ratio Zn/Co; 0.18%Co, 16.81%Zn with 99 ratio Zn/Co and 0.20%Co, 16.76%Zn with 74 ratio Zn/Co ). These values are not even detected by the EDS analyses. With equimolar amounts of zinc and cobalt, TMPF-90 is again observed in the PXRD pattern, mixed with TMPF-88 (Figure S10). A further increase in the amount of cobalt (Zn:Co 1:2) results in the appearance of a new phase, TMPF-95. TMPF-90 is still present according to the PXRD patterns, although as a minor phase. The Zn:Co ratio for TMPF-95 crystals according to EDS analysis is 1:2 (Figure 11), which is coincident with the initial ratio of the reactants. Yield and purity of this phase increase when the reaction is carried out for a 3 days period. A single crystal X-ray diffraction analysis was carried out for a Zn-Co-TMPF-95. In this crystal structure there are five crystallographically independent metal

atoms, three of them in tetrahedral coordination environment, and two of them octahedrally coordinated. Despite the similar electron density of cobalt and zinc, we attempted to assign the different metal positions to both elements, to ascertain whether there is an ordered metal distribution. The results of the structural refinements indicate that this is not the scenario, but on the contrary, the two metal cations should be randomly distributed in the SBUs along the crystal. Indeed, the best refinement indicators were obtained when all five metal positions were assigned as cobalt, as expected as this is the element in a larger amount according to the spectroscopic analysis.

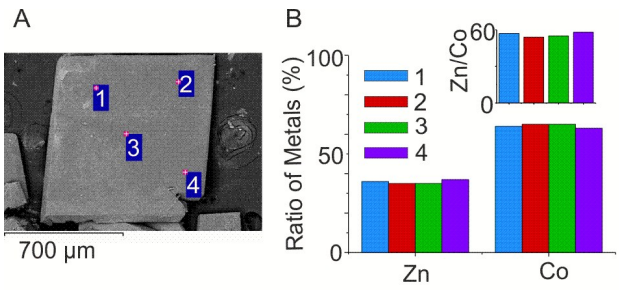


Figure 11. SEM images corresponding to TMPF-95 crystals, indicating the areas where the EDS analyses were performed. A) Sample prepared with an initial 10:1 Zn:Co ratio. B) Plot of the ratio of metals (%) and Zn/Co ratio determined by EDS analysis, where each column corresponds to the area indicated by a number in panel A. C) Sample prepared with an initial 8:1 Zn:Co ratio. D) Plot of the ratio of metals (%) and Zn/Co ratio determined by EDS analysis, where each column corresponds to the area indicated by a number in panel C.

With a further increase in the amount of cobalt in the synthesis mixture, and for Zn:Co ratios of 1:4, 1:10 and 0:1, crystals of the Co(hfipbb)($H_2$fipbb)$_{0.5}$ phase area again formed along with a yellowish powder, similar to what we observed in the water:ethanol system.

## Conclusions

In summary, in this work we have shown that the addition of a second metal element, even at a very low amount, drastically modifies the reaction media, inducing the formation of new phases, as shown by the formation of TMPF-91 with a 10:1 Zn:Co intial ratio. Furthermore, in the mixed-metal, mixed-ligand system here studied, there is a competition in MOF formation, where kinetically favoured structures (ZnPF-1 and TMPF-90) appear at short reaction times, precluding the obtaining as pure phase of other energetically more favourable solid-solution phases (TMPF-88). In addition, another MOF was isolated (TMPF-95), which could be prepared only with a very specific Zn:Co ratio (1:2). Despite the restricted amount required for preparing this phase, the single crystal X-ray diffraction analysis indicates that the two metal cations are disorderly disposed occupying different crystallographic sites. EDS and ICP analyses demonstrate that solid-solution phases can be obtained, although the amount of cobalt incorporated into the framework is substantially lower than the one initially added to the reaction in the cases of TMPF-91 and TMPF-88, while in the case of TMPF-90 and TMPF-95, the two elements can be incorporated in comparable amounts.

## Acknowledgements

This work has been supported by the Spanish Ministry of Economy and Competitiveness, project MAT2013-45460-R. Financial support by Fundación General CSIC (Programa ComFuturo) is acknowledged (F.G.). Computational time has been provided by the Centre de Supercomputació de Catalunya (CESCA) We thank E. Rodríguez-Cañas from the Servicio Interdepartamental de Investigación (SIdI) at Universidad Autónoma de Madrid for valuable support with SEM images and EDS analyses acquisition.

## Notes and references

1. H. Furukawa, K. Cordova, M. O'Keeffe and O. Yaghi, *Science*, 2013, **341**, 974-986.
2. M. Li, D. Li, M. O'Keeffe and O. M. Yaghi, *Chem. Rev.*, 2014, **114**, 1343-1370.
3. H. Furukawa, U. Müller and O. M. Yaghi, *Angew. Chem. Int. Ed.*, 2015, **54**, 3417-3430.
4. H. X. Deng, C. J. Doonan, H. Furukawa, R. B. Ferreira, J. Towne, C. B. Knobler, B. Wang and O. M. Yaghi, *Science*, 2010, **327**, 846-850.
5. J. M. Taylor, S. Dekura, R. Ikeda and H. Kitagawa, *Chem. Mat.*, 2015, **27**, 2286-2289.
6. O. Karagiaridi, N. A. Vermeulen, R. C. Klet, T. C. Wang, P. Z. Moghadam, S. S. Al-Juaid, J. F. Stoddart, J. T. Hupp and O. K. Farha, *Inorg. Chem.*, 2015, **54**, 1785-1790.
7. Z. Fang, J. P. Dürholt, M. Kauer, W. Zhang, C. Lochenie, B. Jee, B. Albada, N. Metzler-Nolte, A. Pöppl, B. Weber, M. Muhler, Y. Wang, R. Schmid and R. A. Fischer, *J. Am. Chem. Soc.*, 2014, **136**, 9627-9636.
8. M. J. Cliffe, W. Wan, X. Zou, P. A. Chater, A. K. Kleppe, M. G. Tucker, H. Wilhelm, N. P. Funnell, F. X. Coudert and A. L. Goodwin, *Nat. Commun.*, 2014, **5**.
9. H. Wu, Y. S. Chua, V. Krungleviciute, M. Tyagi, P. Chen, T. Yildirim and W. Zhou, *J. Am. Chem. Soc.*, 2013, **135**, 10525-10532.
10. D. Britt, H. Furukawa, B. Wang, T. G. Glover and O. M. Yaghi, *Proc. Natl. Acad. Sci. U. S. A.*, 2009, **106**, 20637-20640.
11. T. M. McDonald, J. A. Mason, X. Kong, E. D. Bloch, D. Gygi, A. Dani, V. Crocellà, F. Giordanino, S. O. Odoh, W. S. Drisdell, B. Vlaisavljevich, A. L. Dzubak, R. Poloni, S. K. Schnell, N. Planas, K. Lee, T. Pascal, L. F. Wan, D. Prendergast, J. B. Neaton, B. Smit, J. B. Kortright, L. Gagliardi, S. Bordiga, J. A. Reimer and J. R. Long, *Nature*, 2015, **519**, 303-308.
12. J. Lee, O. K. Farha, J. Roberts, K. A. Scheidt, S. T. Nguyen and J. T. Hupp, *Chem. Soc. Rev.*, 2009, **38**, 1450-1459.
13. F. Gándara, F. J. Uribe-Romo, D. K. Britt, H. Furukawa, L. Lei, R. Cheng, X. F. Duan, M. O'Keeffe and O. M. Yaghi, *Chem.-Eur. J.*, 2012, **18**, 10595-10601.
14. L. Sun, C. H. Hendon, M. A. Minier, A. Walsh and M. Dincă, *J. Am. Chem. Soc.*, 2015, **137**, 6164-6167.
15. C. K. Brozek and M. Dincă, *Chem. Soc. Rev.*, 2014, **43**, 5456-5467.
16. B. Tu, Q. Pang, D. Wu, Y. Song, L. Weng and Q. Li, *J. Am. Chem. Soc.*, 2014, **136**, 14465-14471.
17. L. J. Wang, H. Deng, H. Furukawa, F. Gándara, K. E. Cordova, D. Peri and O. M. Yaghi, *Inorg. Chem.*, 2014, **53**, 5881-5883.
18. R. F. D'Vries, S. Alvarez-Garcia, N. Snejko, L. E. Bausa, E. Gutierrez-Puebla, A. de Andres and M. A. Monge, *J. Mater. Chem. C*, 2013, **1**, 6316-6324.
19. L. Mitchell, P. Williamson, B. Ehrlichov, A. E. Anderson, V. R. Seymour, S. E. Ashbrook, N. Acerbi, L. M. Daniels, R. I. Walton, M. L. Clarke and P. A. Wright, *Chem.-Eur. J.*, 2014, **20**, 17185-17197.

20. L. M. Aguirre-Díaz, F. Gándara, M. Iglesias, N. Snejko, E. Gutiérrez-Puebla and M. Á. Monge, *J. Am. Chem. Soc.*, 2015, **137**, 6132-6135.
21. G. M. Sheldrick, *Acta Crystallogr. Sect. A*, 2008, **64**, 112-122.
22. O. V. Dolomanov, L. J. Bourhis, R. J. Gildea, J. A. K. Howard and H. Puschmann, *J. Appl. Crystallogr.*, 2009, **42**, 339-341.
23. G. Kresse and J. Furthmüller, *Comput. Mater. Sci.*, 1996, **6**, 15-50.
24. G. Kresse and J. Hafner, *Physical Review B*, 1993, **47**, 558-561.
25. J. P. Perdew and Y. Wang, *Physical Review B*, 1992, **45**, 13244-13249.
26. J. P. Perdew, J. A. Chevary, S. H. Vosko, K. A. Jackson, M. R. Pederson, D. J. Singh and C. Fiolhais, *Phys. Rev. B*, 1992, **46**, 6671-6687.
27. G. Kresse and D. Joubert, *Phys. Rev. B: Condens. Matter Mater. Phys.*, 1999, **59**, 1758-1775.
28. P. E. Blöchl, *Phys. Rev. B*, 1994, **50**, 17953-17979.
29. A. Monge, N. Snejko, E. Gutierrez-Puebla, M. Medina, C. Cascales, C. Ruiz-Valero, M. Iglesias and B. Gomez-Lor, *Chem. Commun.,* 2005, 1291-1293.
30. F. Gándara, V. A. de la Pena-O'Shea, F. Illas, N. Snejko, D. M. Praserpio, E. Gutierrez-Puebla and M. A. Monge, *Inorg. Chem.*, 2009, **48**, 4707-4713.
31. M. C. Bernini, V. A. de la Peña-O'Shea, M. Iglesias, N. Snejko, E. Gutierrez-Puebla, E. V. Brusau, G. E. Narda, F. Illas and M. Á. Monge, *Inorg. Chem.*, 2010, **49**, 5063-5071.
32. A. E. Platero-Prats, V. A. de la Pena-O'Shea, D. M. Proserpio, N. Snejko, E. Gutierrez-Puebla and A. Monge, *J. Am. Chem. Soc.*, 2012, **134**, 4762-4771.
33. R. F. D'Vries, V. A. de la Pena-O'Shea, N. Snejko, M. Iglesias, E. Gutierrez-Puebla and M. Angeles Monge, *J. Am. Chem. Soc.*, 2013, **135**, 5782-5792.
34. R. F. D'Vries, V. A. de la Peña-O'Shea, Á. Benito Hernández, N. Snejko, E. Gutiérrez-Puebla and M. A. Monge, *Cryst. Growth Des.*, 2014, **14**, 5227-5233.
35. H.-L. Jiang and Q. Xu, *CrystEngComm*, 2010, **12**, 3815-3819.

**Table of contents**

Addition of small amounts of a second metal cation results in crystal phase competition during the synthesis of solid-solution MOFs.